Journal of Applied Polymer Science

Adhesion of Maleic Anhydride Functionalized Polyolefins and Blends

Mun Fu Tse
ExxonMobil Chemical Company, Baytown, Texas 77520
Correspondence to: M. F. Tse (E-mail: munfu1999@yahoo.com)

ABSTRACT: We study three new classes of olefin-based polymer, low-molecular-weight homopolypropylene (LMW-hPP), syndiotactic-rich polypropylene (srPP), and random propylene polymer (RPP). RPP is a random propylene/ethylene copolymer. By blending LMW-hPP with 20 wt % of a maleic anhydride (MA) functionalized srPP (MA-srPP) or MA functionalized RPP (MA-RPP) instead of a commercial MA-iPP (maleic anhydride-*grafted*-isotactic polypropylene), adhesion to a polar substrate, such as polyester (Mylar), is greatly enhanced. Effects of crystallinity controlled by either stereoregularity or comonomer incorporation and molecular weight of these MA functionalized propylene-based polymers on adhesive performance are discussed. To further understand the mechanisms of enhanced adhesion, Sum Frequency Generation (SFG) spectroscopy is used to evaluate the migration of MA-srPP in LMW-hPP towards the interface when contacting a polar sapphire substrate. It shows that the buried interface between the LMW-hPP/MA-srPP blend (wt ratio = 80/20) and sapphire has the same characteristic spectrum as the MA-srPP/sapphire interface, suggesting the enrichment of MA-srPP in the interfacial polymer when the blend is in contact with sapphire. Also, vibrational modes of C=O have been detected at both the blend/sapphire and MA-srPP/sapphire interfaces, further indicating that the interfacial polymer contains MA groups. Besides Mylar, adhesion to the non-polar iPP substrate is also studied. The adhesion mechanisms to these polar and non-polar substrates are explained in terms of our adhesion model. Applications of these MA functionalized polyolefins and blends are envisioned in the tie-layer and adhesive areas. © 2013 Wiley Periodicals, Inc. J. Appl. Polym. Sci. **2014**, *131*, 39855.

KEYWORDS: adhesives; blends; copolymers; functionalization of polymers; polyolefins

Received 30 March 2013; accepted 27 July 2013
DOI: 10.1002/app.39855

INTRODUCTION

Interfaces are always present in fabricated polymer products and their compositions affect properties. For one polymer bonded to the other, the joint separation force (P) demands the transfer of the mechanical stress through the interface. First, the effectiveness of this transfer depends on the molecular interactions across the interface (P_o). Second, with a non-zero value of P_o, P can further be improved by the optimization of the bonding term (B) so that the interface can sustain sufficient amount of stress to induce energy absorption, such as viscous flow, yield, cavitation or crazing, in the bulks. Third, P can further be enhanced by the debonding term (D) as described by the aforementioned energy dissipation (bulk deformation). More specifically, D represents the energy dissipated plastically and viscoelastically in the highly strained element in the vicinity of the propagating crack or the peel front and in the body of the joint, e.g., in bending a flexible substrate. Therefore, this term will contribute to the rate and temperature dependence of joint strengths. Normally the D term dominates the measured adhesion. All these P_o, B, and D terms are described and illustrated by the adhesion model [Figure 1 and eq. (1)].[1–3]

$$P = P_o BD \tag{1}$$

Therefore, the joint or bond strength is governed by the interplay between the thermodynamic work of adhesion for producing newly debonded surfaces by rupture and the fracture mechanics of the interfacial system. Surface chemistry or composition influences the fracture mechanics of the adhesive joint. Due to the multiplicative nature of eq. (1), a two-fold increase in P_o will result in a two-fold increase in adhesion if B and D remain constant. This is the major reason that, even if the bulk properties of two adhesives are similar, a change in the interfacial properties of the adhesive will affect adhesion.

Because of their attributes of chemical inertness, low density and low cost, olefin-based polymers are widely used in various applications, such as adhesives, tie layers, films, fibers, automotive, construction, appliances, etc. However, bond strength of olefin-based polymer with some substrates, especially the more

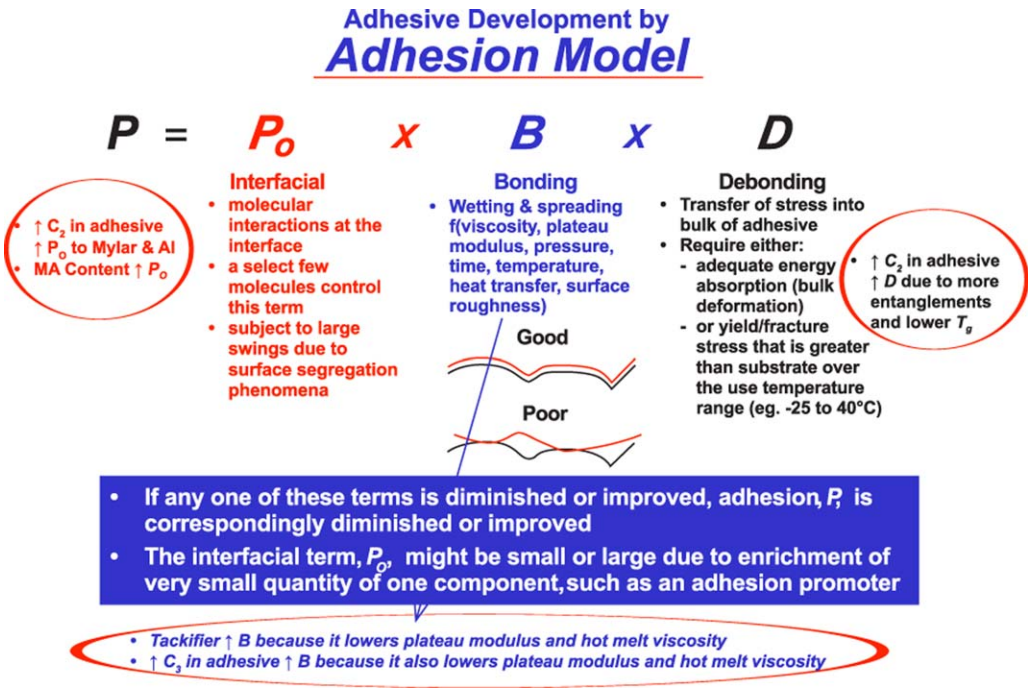

Figure 1. Adhesion model. [Color figure can be viewed in the online issue, which is available at wileyonlinelibrary.com.]

polar ones, such as polyester, corona-discharge-treated polyolefin, ionomer, nylon, poly(vinyl alcohol), poly(vinylidene chloride), polycarbonate, paper cardboard, metals, glass, etc., is generally low. This study describes a novel way to modify or improve the P_o term of a propylene-based polymer, LMW-hPP, with the use of MA functionalized srPPs or RPPs instead of a commercial MA-iPP. We have studied ethylene-based copolymers used as adhesives.[2,4] However, propylene-based polymers have certain merits in the performance of adhesive compositions because of its lower plateau modulus (~0.43–1.35 MPa and 2.60 MPa for polypropylene and polyethylene, respectively), higher T_g (−10°C and −128°C for polypropylene and polyethylene, respectively), and higher melting temperature (T_m).[5–7] The first attribute improves hot melt bonding and processability (Figure 1). The second attribute enhances the cohesion of an adhesive. Generally, the observed strength or cohesion is governed by the polymer chain segmental viscosity. Therefore, the cohesion of two polymers is compared by normalizing the test temperature and polymer T_g in order to minimize the contribution from differences in viscoelasticity. The third attribute elevates the high-temperature resistance of the adhesive. Of course, similar to a homopolymer of ethylene, a homopolymer of propylene is not an optimum base polymer for adhesives. One wants to improve adhesion by (1) blending into another polymer component, such as an adhesion promoter, bonding or debonding modifier, etc. (Figure 1), (2) copolymerizing propylene with ethylene or another alpha-olefin, or (3) doing both. For example, copolymerizing certain amounts of ethylene in a propylene-based polymer should decrease the yield stress. Also, it should increase the surface energy because polyethylene has a higher surface energy than polypropylene.[8] All the above approaches are being explored and studied in this study.

Table I. Polymers and Abbreviations

Abbreviation	Description	Function
PP	Polypropylene	Polymer
aPP	Atactic PP	Polymer
LMW-hPP	Low Molecular Weight Homopolypropylene	Base Polymer
iPP	Isotactic PP	Substrate, Polymer Precursor
sPP	Syndiotactic PP	Polymer
MA-iPP	Maleic Anhydride Functionalized iPP	Polymer Modifier
srPP	Syndiotactic-Rich PP	Polymer Modifier, Polymer Precursor
MA-srPP	Maleic Anhydride Functionalized srPP	Polymer Modifier
RPP	Random Propylene Polymer	Polymer Modifier, Polymer Precursor
MA-RPP	Maleic Anhydride Functionalized RPP	Polymer Modifier

Polypropylene (PP) properties primarily depend on tacticity, molecular weight, and molecular weight distribution. Abbreviations of polymer used in this study are shown in Table I. According to tacticity or stereoregularity, PP can be divided into isotactic-PP (iPP), atactic-PP (aPP), and syndiotactic-PP (sPP). As an excellent example for structure–property relationships, the plateau moduli have been found to be 0.43 MPa for iPP, 0.48 MPa for aPP, and 1.35 MPa for sPP.[5] This effect of stereoregularity on plateau modulus has been attributed to the different conformations of sPP with respect to iPP and aPP in PP melts. Also, it has been reported that stereoregularity may be one of the dominant factors to control the thermal stability of PP. Compared to iPP, sPP may suffer less chain scission in heat treatments carried out in air at 160–220°C for 10–30 min.[9]

MA functionalized polymers have been used as compatibilizers or in dispersed phases in polymer blends or composites for improving mechanical properties.[10–17] To the best of our knowledge, there have been only a few systematic studies on the adhesion of MA functionalized polymers with another polymer. It was found that natural rubber modified by MA improved the peel strength between ethylene/propylene/diene monomer (EPDM) terpolymer and polyester fabric.[18] It was also observed that, when a thin layer of styrene/maleic anhydride random copolymer was introduced between the sheets of immiscible amorphous polyamide and polystyrene, the interfacial fracture toughness of the annealed joined polymers measured by an asymmetric fracture test was increased.[19]

This work studies and compares three different MA functionalized propylene-based polymers used as adhesion modifiers or promoters. Two of them are based on our new polyolefins: srPP and RPP. The third one is a commercial MA-iPP. We investigate the blending effects of these functionalized polymers of different crystallinities and molecular weights on the adhesion of LMW-hPP to either a polar substrate, polyester, or to a non-polar substrate, iPP. Polyolefin crystallinity is controlled either by stereoregularity with catalyst selection or by comonomer incorporation. Also, the adhesion of the neat MA functionalized srPPs and RPPs to the above substrates is measured. Applications of these MA functionalized polyolefins and blends could be in the tie-layer and adhesive areas. One of our objectives is to understand the content of functional group, crystallinity, and molecular weight of MA functionalized polymers for improving/modifying the adhesion and surface properties of LMW-hPP. The other objective is to prove our adhesion model [eq. (1) and Figure 1] can be used to guide adhesive development.

EXPERIMENTAL AND CHARACTERIZATION

Size Exclusion Chromatograph

Molecular weights of each polymer were determined using a Waters 150 Size Exclusion Chromatograph (SEC) equipped with a differential refractive index (DRI) detector, an online low angle light scattering (LALLS) detector, and a viscometer (VIS). The details of the detector calibrations and experimental procedures have been described elsewhere.[20] The SEC was equipped with three PLgel 10 μm Mixed-B columns from Polymer Laboratories, UK, for separation using a flow rate of 0.54 mL/min and a nominal injection volume of 300 μL. The various transfer lines, columns and the DRI detector were contained in an oven maintained at 135°C. The LALLS detector (Model 2040 dual-angle light scattering photometer, Precision Detector Inc.) was placed after the SEC columns, but before the viscometer. The viscometer (a high temperature Model 150R, Viscotek Corporation) was placed inside the SEC oven, positioned after the LALLS detector but before the DRI detector. The permeation solvent was 1,2,4-trichlorobenzene. The polymer concentration was ~1–4 mg/mL, with lower concentrations being used for polymers with higher molecular weights. The g' index was measured using SEC with the on-line viscometer (SEC-VIS). The g' index is defined as η_b/η_b where η_b is the intrinsic viscosity of the branched polymer and η_l is the intrinsic viscosity of a linear polymer of the same viscosity-averaged molecular weight (M_v) as the branched polymer.

MA Content

A method described by Sclavons et al.[21] was used to determine the MA contents of all MA functionalized polymers. Approximately 0.5 g of the polymer was dissolved in 150 mL of toluene at boiling temperature. A potentiometric titration with TBAOH (tetra-butylammonium hydroxide) using bromothymol blue as the color indicator was performed on the heated solution in which the polymers did not precipitate during titration.

DSC Measurements

In the TA Instruments Model 2920 DSC, samples were first heated to 200°C at a rate of 10°C/min and held at 200°C for 5 min. They were then cooled to −50°C at a rate of 20°C/min and held at −50°C for 5 min. Finally, they were heated again to 200°C at a rate of 10°C/min. All runs were carried out in a nitrogen environment. The values of crystallization temperature (T_c), T_m, T_g, and heat of fusion (ΔH_u) were reported based on DSC second melt.

Solid-State NMR Measurements

Solid-state NMR measurements were performed in a Bruker DSX 500 spectrometer, with a ^{13}C resonance frequency of 126.76 MHz, as a means of determining the C_2 contents of various RPPs and MA-RPPs. A ^{13}C direct polarization/high-power ^{1}H decoupling pulse sequence was used. Spectra were acquired at 60°C or higher to ensure most of the crystallites were melted. Recycle time was 20 s. The method may have a systematic error of up to 1 wt %.

LMW-hPP

The propylene-based polymers (also denoted as aPP-iPP), prepared with metallocene catalysts, are described in Table II, where η is the Brookfield viscosity at 190°C measured according to ASTM D 3236. ΔH_u of each polymer is a measure of crystallinity. For crystalline PP, ΔH_u is 8.7 kJ/mol or 207 J/g.[22] The value of ΔH_u of each LMW-hPP in Table II divided by 207 J/g can be considered as the degree of crystallinity. Therefore, LMW-hPP-1, −2, and −3 have similar degree of crystallinity, whereas LMW-hPP-4, −5, −6, and −7 are less crystalline. The g' is the branching parameter or index.[20] A lower g' suggests a higher concentration of branching in the polymer.

Table II. Characterization of LMW-hPP

LMW-hPP-	1	2	3	4	5	6	7
M_n/1000	13.0	15.2	20.4		19.6	13.1	18
M_w/1000	37.6	45.2	55.0		41.1	29.3	48
M_z/1000	64.0	81.0	94.6		76.0	62.6	83
g'	0.93	0.95	0.93		0.88	0.99	
T_c (°C)	88	90	92	80	78	68	86
T_m (°C)	127	138	141	139	132	136	138
T_g (°C)	−6	−5	−4			−6	−4
ΔH_u (J/g)	37	38	38	32	29	22	30
190°C η (Pa s)	1.9	4.0	11	2.4	1.6	1.5	6.0

srPP and Functionalized srPP

The precursor polymers for functionalized srPPs were prepared with metallocene catalysts. These srPPs have $m/r < 1$, r dyads ~ 58–75%, and no crystallinity (Tables III and IV). The designation, m or r, describes the stereochemistry of pairs of contiguous propylene groups, m referring to meso and r to racemic. The m/r value, known as the propylene tacticity index, is determined by ^{13}C nuclear magnetic resonance (NMR) and calculated as defined by Cheng.[23] An m/r of 0 to less than 1.0 generally describes an sPP, and an $m/r = 1.0$ an aPP, and an $m/r > 1.0$ an iPP. An iPP theoretically may have a ratio approaching infinity, and many by-product aPPs have sufficient isotactic content to result in $m/r > 50$.

Functionalization of srPP was carried out by dissolving 120 g of srPP in toluene (polymer concentration: 20 wt %). Maleic anhydride used was 15 wt % based on srPP. The radical initiator, 2,5-dimethyl-2,5-di(*t*-butylperoxyl)hexane, was 2.5 wt % based

Table III. Triad and Diad mol %'s of srPP

srPP-	mm	mr + rm	rr	*m*	*r*	*m/r*
3	15	48	37	39	61	0.64
4	13	46	40	37	63	0.59
5	11	44	45	33	67	0.49
6	9	40	51	29	71	0.41

Table IV. Characterization of srPP, MA-srPP, MA-iPP, RPP, and MA-RPP

Polymer	Mol % (wt %) C_2	$M_n/10^3$	$M_w/10^3$	$M_z/10^3$	M_w/M_n	$\Delta M_w/M_w$	g'	wt % MA	mm (%)	T_g (°C)	T_m (°C)	ΔH_u (J/g)
srPP-1	0	23	62	148	2.70		1.08	0				
MA-srPP-1	0	8	20	38	2.50	0.68		3.20		−14		0
srPP-3	0	17	43	80	2.53		0.98	0	15	−4		0
MA-srPP-3	0	17	33	55	1.94	0.23		1.92		−5		0
srPP-4	0	34	86	177	2.53		1.05	0	13	0		0
MA-srPP-4	0	23	44	71	1.91	0.49		1.00		0		0
srPP-5	0	74	188	385	2.54		1.11	0	11	−1		0
MA-srPP-5	0	29	68	116	2.34	0.64		1.00		−1		0
srPP-6	0	128	311	606	2.43		1.19	0	9	1		0
MA-srPP-6	0	60	135	263	2.25	0.57		1.12		0		0
MA-iPP	0	3.7	9.8	18	2.65			5.24			150	58
RPP-1	21.6 (15.5)	142	249	384	1.75			0	91	−28	44	11
MA-RPP-1	20.8 (14.9)	19	88	140	4.63	0.65		1.17		−32	56	14
RPP-2	20.9 (15.0)	82	136	200	1.66			0	88	−27	45	14
RPP-3	15.6 (11.0)	98	162	240	1.66			0	90	−18	73	40
MA-RPP-4	20.1 (14.4)	16	66	103	4.13			1.98		−31	55	10
MA-RPP-5	15.2 (10.7)	17	74	116	4.35			1.92		−27	73	43

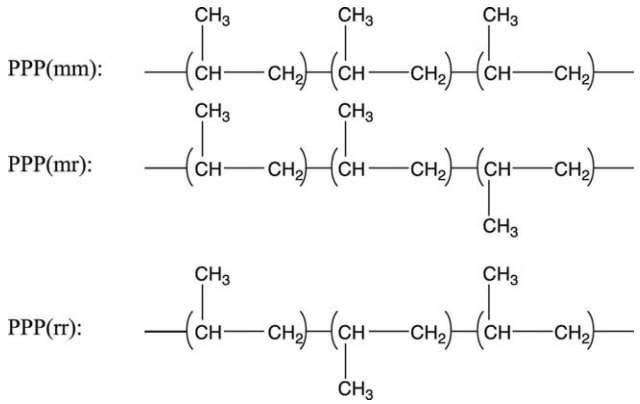

Scheme 1. Schematic diagram illustrating triad sequences.

on srPP. The reaction temperature was 139°C and the reaction time was 4 h. The srPP-i represents the precursor polymer of the MA-srPP-i, where $i = 1$, 3, 4, 5, or 6. After functionalization, molecular weights were decreased in all cases (Table IV). To compare the performance of functionalized srPP-i's to their non-functionalized counterparts, the lowest molecular weight srPP-3 polymer was used as a control. Even though srPP-3 has molecular weights (M_n, M_w, and M_z) approximately two times higher than MA-srPP-1, we choose srPP-3 as the control because its molecular weights are closer to MA-srPP-1 than srPP-1.

RPP and Functionalized RPP

The RPPs used in this study have the ratio $m/r > 1$ and isotactic stereoregular propylene crystallinity. The term "stereoregular" used here means that the predominant number, i.e., greater than 80%, of the propylene residues in the polypropylene exclusive of any other monomer such as ethylene, has the same 1,2-insertion and the stereochemical orientation of the pendant methyl groups is the same, either *m* or *r*. Each RPP has an mm triad tacticity of three propylene units, as measured by ^{13}C NMR, of 75% or greater (Table IV). The mm triad tacticity of a polymer is the relative tacticity of a sequence of three adjacent propylene units, a chain consisting of head to tail bonds, expressed as a binary combination of *m* and *r* sequences. It is usually expressed for semi-amorphous copolymers as the ratio of the number of units of the specified tacticity to all of the propylene triads in the copolymer. The mm triad tacticity (mm fraction) of a propylene copolymer can be determined from a ^{13}C NMR spectrum of the propylene copolymer and the following formula:

$$\text{mm Fraction} = \frac{\text{PPP(mm)}}{\text{PPP(mm)} + \text{PPP(mr)} + \text{PPP(rr)}}$$

where PPP(mm), PPP(mr), and PPP(rr) denote peak areas derived from the methyl groups of the second units in the three propylene unit chains consisting of head-to-tail bonds shown in Scheme 1.

The ^{13}C NMR spectrum of the propylene copolymer was measured as described by Imuta et al.[24] The spectrum relating to the methyl carbon region (19–23 ppm) can be divided into a first region (21.2–21.9 ppm), a second region (20.3–21.0 ppm), and a third region (19.5–20.3 ppm). Each peak in the spectrum was assigned with reference the methods described by Cheng[23] and Tsutsui et al.[25] In the first region, the methyl group of the second unit in the three propylene unit chain represented by PPP (mm) resonates. In the second region, the methyl group of the second unit in the three propylene unit chain represented by PPP (mr) resonates, and the methyl group (PPE-methyl group) of a propylene unit whose adjacent units are a propylene unit and an ethylene unit resonates (in the vicinity of 20.7 ppm). In the third region, the methyl group of the second unit in the three propylene unit chain represented by PPP (rr) resonates, and the methyl group (EPE-methyl group) of a propylene unit whose adjacent units are ethylene units resonates (in the vicinity of 19.8 ppm). The calculation of the triad tacticity was outlined in the techniques by Imuta et al.[24] By subtracting the peak areas for the error in propylene insertions (both 2,1 and 1,3) from peak areas from the total peak areas of the second region and the third region, the peak areas based on the three propylene unit chains (PPP(mr) and PPP(rr)) consisting of head-to-tail bonds can be obtained. Thus, the peak areas of PPP(mm), PPP(mr), and PPP(rr) can be evaluated, leading to the determination of the mm triad tacticity of the propylene unit chain consisting of head-to-tail bonds.

Functionalization of RPP was carried out in a non-intermeshing counter-rotating twin screw extruder by using the following conditions: 97.5–98.5 wt % of polymer, 1.5–2.5 wt % of Crystalman™ maleic anhydride fed at a rate of 7 kg/h to the hopper of the extruder, and 0.24–0.40 wt % of a 10% solution of Luperox™ 101 dissolved in Marcol™ 52 oil added to the second barrel.[26] The screw speed was set at 125 rpm and the following temperature profile was used: 180, 190, 190, 190°C with the die at 180°C. Excess reagents as well as peroxide decomposition products were removed with vacuum and heat prior to the recovery of the polymer. Characterization of RPPs and MA-RPPs is shown in Table IV. The precursor polymer for MA-RPP-1 is RPP-1. The precursor polymer for MA-RPP-4 is a lower-ethylene-content RPP (~14 wt % C_2 instead of ~15 wt % C_2). The precursor for MA-RPP-5 is an RPP with an even lower wt % C_2.

MA-iPP

The MA-iPP studied is POLYLETS® MAPP 40 from CHUSEI Inc. Some properties of this polymer are shown in Tables IV and V. This commercial MA-iPP has a higher MA content and

Table V. Characterization of MA-iPP

Typical properties		Remark
Softening Point, ASTM D 36, °C	143–155	CHUSEI
190°C η (Pa s)	~0.4	CHUSEI
Acid value	45–50	CHUSEI
T_c (°C)	104	This study
T_m (°C)	150	This study
ΔH_u (J/g)	58	This study
$M_n/10^3$	3.7	This study
$M_w/10^3$	9.8	This study
$M_z/10^3$	18	This study

a higher degree of crystallinity than each MA-srPP or MA-RPP. As a summary of the degrees of crystallinity of the various MA functionalized propylene-based polymers in this study, ΔH_u increases in the following order: MA-iPP > MA-RPP > MA-srPP (Table IV).

Formulations and Peel Adhesion Measurements

Blends of LMW-hPP with srPP, MA-srPP, RPP, MA-RPP, or MA-iPP were mixed thoroughly and homogeneously in the thermal cell of a Brookfield viscometer equipped with an electrically driven stirrer at 180°C. For the majority of blend compositions studied in this work, two formulations were used: LMW-hPP/srPP, MA-srPP, or MA-iPP = 80/20 and LMW-hPP/E-5380/srPP, MA-srPP, RPP, MA-RPP or MA-iPP = 72/8/20 in wt ratio, where E-5380 denotes Escorez™ 5380 tackifying resin, a water white hydrogenated oligocyclopentadiene hydrocarbon tackifier with $M_w = 440$, $M_w/M_n = 1.83$, and DSC $T_g = 36$°C.[27,28] This tackifier was used because it is compatible with the propylene-based polymers, such as iPP.[29–31] After mixing, blends were degassed in a vacuum oven at 180°C and subsequently cooled down to 25°C. This was performed for each blend before molding and bonding to eliminate the possibility of air bubbles in the subsequent fabrication of the adhesive layer. Each blend was then molded into a thin sheet of material with thickness about 0.4 mm at 180°C for 10 s. For the preparation of the T-peel specimens, this thin sheet of adhesive sample was laminated between two pieces of Mylar substrate (0.003" = 0.076 mm thickness; used as received) in a positive pressure, Teflon-coated mold at a temperature of 180°C and a pressure of 0.67 MPa for 10 s. For the iPP substrate (polymerized from a metallocene catalyst; melt flow rate = 9 dg/min measured by ASTM D 1238 at 230°C under a load of 2.16 kg; $T_m = 152$°C), a lower bonding temperature of 150°C was used. All these adhesive/substrate laminates were cut into 1/2" = 1.3 cm wide specimens. The adhesive thickness was ~0.2–0.3 mm. T-peel measurements using triplicate samples (bonds conditioned for 12 h before peel unless otherwise specified) were performed at room temperature and at a separation speed of 2"/min = 850 μm/s in an Instron Tester. Adhesion was measured by the average work of detachment (identical to the adhesive fracture energy, G_a, which is equal to twice the peel strength):

$$G_a = \quad 2F/w$$

where F is the peel force and w is the width of the test specimen.

Stress–Strain Measurements

The polymer or blend was molded at 180°C for 10 s into a pad with a thickness ~0.4 mm. The test specimen, a small dumbbell (the base is ~1 cm × 1 cm and the center, narrow strip is ~0.6 cm × 0.2 cm), was die-cut from the molded pad. Measurements using triplicate samples were performed at room temperature and at a separation speed of 2"/min = 850 μm/s in an Instron Tester. Nominal stress and strain based on clamp separation were used.

SFG Measurements

The generation of sum frequency photons does not occur in the bulk of a centrosymmetric material, such as a polymer or a solid substrate. However, it happens at an interface or surface where the inversion symmetry is lifted. This intrinsic property of sum frequency generation (SFG) along with its high sensitivity to molecular species make the SFG spectroscopy an ideal tool to study the molecular arrangement and migration of polymer functional group towards an interface. This technique has been used to characterize the surface of a terpolymer (BIMSM) of isobutylene, *p*-bromomethylstyrene, and *p*-methylstyrene and ensure the existence of crosslinkable species, the *p*-bromomethylstyrene functional group, on this polymer.[32]

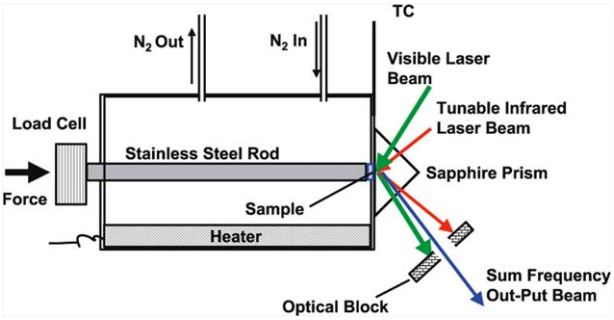

Figure 2. Schematic diagram depicting the SFG instrument. [Color figure can be viewed in the online issue, which is available at wileyonlinelibrary.com.]

The measurements were performed using a spectrometer designed and assembled within our company. The optical setup briefly consisting of a nanosecond Spectral Physic Nd : YAG laser and a multi-pass hydrogen Raman shifter is described elsewhere.[33,34] A portion of the output of the doubled-Nd : YAG laser was used as the visible light source. The incident light pulses had a duration of ~7 ns and an intensity of ~10/cm^2 for both the visible and infrared beams, which was at least an order of magnitude below the measured sample damage threshold. The vibrational modes corresponding to the symmetric and asymmetric stretches of CH_3, CH_2, and C=O were excited using a tunable infrared laser beam with a photon energy of 2800–3100 and 1650–1900 cm^{-1}. These excitations were combined with optical transitions, caused by a visible laser beam, to produce SFG resonance signals which are indicative of the interfacial molecules containing the above functionalities. Figure 2 shows the schematic of the instrument. A small amount of polymer (~10 mg) was pressed onto a sapphire (alumina) prism using a stainless steel rod with a pressure of ~0.2 MPa. The sample was heated to 160–170°C for 1 h. The heat was disconnected and the sample was allowed to reach to room temperature. All spectra were collected at room temperature and all the above procedures were carried out under N_2 flow.

RESULTS AND DISCUSSION

Molecular Weight Change of MA-srPP and MA-RPP

Table IV shows the changes in molecular weights and M_w/M_n values of srPP and RPP after maleation. Molecular weights are decreased and MWD (M_w/M_n) narrows for srPP but broadens for RPP after functionalization.

Bond Strength with Mylar for Compositions without Tackifier

Table VI shows the adhesion to Mylar for compositions based on LMW-hPP-1, LMW-hPP-2, and LMW-hPP-3 modified by

Table VI. Adhesion of Compositions Without Tackifier to Mylar

	G_a (J/m^2)	Failure mode
LMW-hPP-1	10.5	AIF
LMW-hPP-1 + 20 wt % srPP-3	35	AIF
LMW-hPP-1 + 20 wt % MA-iPP	66.5	CF
LMW-hPP-2	10.5 ≡ $(G_a)_1$	AIF/CF
LMW-hPP-2 + 20 wt % srPP-3	14	AIF
LMW-hPP-2 + 20 wt % MA-iPP	70	CF
LMW-hPP-2 + 20 wt % MA-srPP-1	424 ~ 40$(G_a)_1$	AIF
LMW-hPP-2 + 20 wt % MA-srPP-3	641	CF/AIF
LMW-hPP-2 + 20 wt % MA-srPP-4	742	AIF
LMW-hPP-2 + 20 wt % MA-srPP-5	2198 ~ 200$(G_a)_1$	CF/AIF
LMW-hPP-2 + 20 wt % MA-srPP-6	1603	AIF
LMW-hPP-3	0.35	AIF
LMW-hPP-3 + 20 wt % srPP-3	7	AIF
LMW-hPP-3 + 20 wt % MA-iPP	112	CF

srPP-3, MA-srPP-1, or MA-iPP. Figure 3(a) illustrates graphically some results for LMW-hPP-2. In Table VI, $(G_a)_1$ is the work of detachment of LMW-hPP-2. The abbreviations, AIF and CF, denote apparent interfacial failure (debonded adhesive left only on one Mylar substrate) and cohesive failure (debonded adhesive left on both Mylar substrates), respectively, as observed visually. Because each T-peel measurement employs triplicate samples, AIF/CF means two samples fail in AIF mode and one sample fails in CF mode. On the other hand, CF/AIF means two samples fail in CF mode and one sample fails in AIF mode. Table VII shows more abbreviations for the failure mode of the adhesive bond. One notes that both Table VI and Figure 3(a) illustrate that MA functional groups of the added modifier improve adhesion of LMW-hPP to Mylar. Also, MA-srPP-1 with a lower MA content but a higher molecular weight outperforms the commercial MA-iPP, demonstrated by LMW-hPP-2 as the base polymer of the adhesive. We think P_o, B, and D in eq. (1) come into the picture at this point. MA content is not the only parameter affecting the P_o term. MA-srPP-1 is amorphous but MA-iPP is semi-crystallized. This may influence the interaction strength for MA-srPP-1 versus MA-iPP with a polar substrate as discussed in the subsequent SFG spectroscopic results. When debonded from Mylar, LMW-hPP-2/MA-srPP-1 fails in AIF mode whereas LMW-hPP-2/MA-iPP fails in CF mode (Table VI). MA-srPP-1 has a higher molecular weight than MA-iPP. Therefore, LMW-hPP-2/MA-srPP-1 should have a higher viscosity than LMW-hPP-2/MA-iPP. Therefore, the former adhesive has a lower B term than the latter adhesive. However, a higher molecular weight of MA-srPP-1 improves the D term of the former adhesive. The strength and failure mode of the adhesive joint will depend on the contributions of these parameters as described by eq. (1) and Figure 1. Further discussions will be continued in the next few sections.

Bond Strength with Mylar for Compositions with Tackifier

Table VIII shows the adhesion to Mylar for blend compositions containing E-5380, where the polymer modifier can be srPP, MA-srPP or MA-iPP. This tackified formulation is LMW-hPP-2/E-5380/polymer modifier = 72/8/20 in wt ratio. Overall, bond strengths are improved compared to the formulations without any tackifier (Figure 4). Table VIII also shows the tremendous increases in bond strength, as high as 4200–4800 J/m^2, for the LMW-hPP-2/E-5380/MA-srPP compositions compared to the formulations containing the precursor srPPs (Figure 5). Therefore, a 1–3 wt % of MA groups in srPP produces a significant increase in adhesion of these adhesives.

To simplify the picture, we produce Figure 3(b) by choosing partial results from Figures 3(a), 4, and 5. It is obvious that, as an adhesion modifier for the LMW-hPP-2 formulations with and without tackifier, MA-srPP-1 is better than either its control without any MA groups, srPP-3, or MA-iPP. Also, except for the case of using MA-iPP as the polymer modifier, all tackified formulations show improved adhesion compared to their counterparts without the tackifier. Discussions in the previous section for the untackified formulations in terms of eq. (1) and

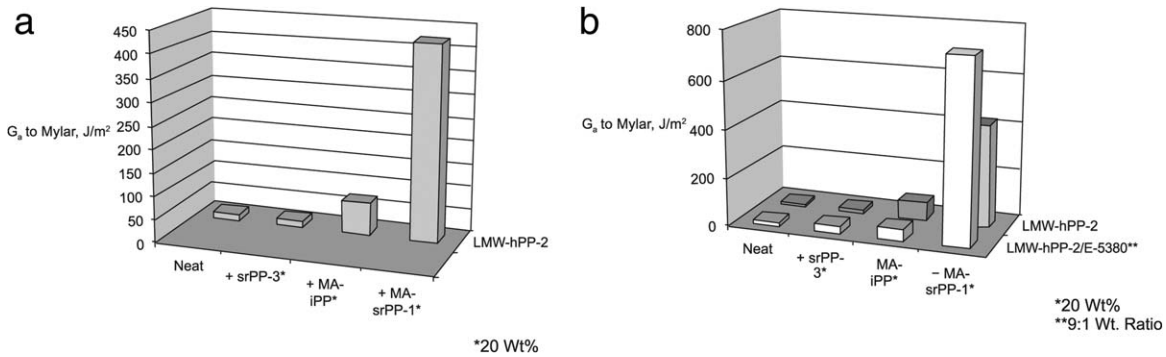

Figure 3. (a) Adhesion of blend of LMW-hPP-2 with srPP, MA-iPP or MA-srPP to Mylar. (b) Improved adhesion of LMW-hPP blend compositions to Mylar by E-5380 tackifier.

Table VII. Abbreviations of Adhesive Failure Mode

Abbreviation	Description
AIF	Apparent Interfacial Failure; debonded adhesive left only on one side of the substrate.
CF	Cohesive failure; debonded adhesive left on both sides of the substrate.
CF/AIF	Two samples fail in CF mode and one sample fails in AIF mode.
AIF/CF	Two samples fail in AIF mode and one sample fails in CF mode.
SE	Substrate Elongated; substrate elongated and bond opened simultaneously.
BRI	Bond Remained Intact; substrate elongated only and eventually broken with no bond separation at all.

Figure 1 are applicable to the tackified formulations in this section. More systematic discussions will be presented in the next section.

At this point, we hypothesize that the contacting polar Mylar substrate may induce migration of MA-srPP to the interface of LMW-hPP modified by MA-srPP. Due to the specific interactions of the MA group of MA-srPP with the C=O group of Mylar, the interfacial adhesion term (P_o) in eq. (1) is enhanced, producing a higher P value or adhesion. Further discussions on the migration of MA-srPP to the interface suggested by SFG measurements and the explanation of the observed adhesion behaviors by eq. (1) will be described in subsequent sections.

Table VIII. Adhesion of Compositions with Tackifier (LMW-hPP-2/E-5380/Polymer Modifier = 72/8/20 wt Ratio) to Mylar

	G_a (J/m^2)	Failure mode
LMW-hPP-2/E-5380 (9 to 1 wt Ratio)	14 $\equiv (G_a)_2$	AIF
LMW-hPP-2/E-5380/srPP-3	31.5	AIF
LMW-hPP-2/E-5380/MA-iPP	49	CF
LMW-hPP-2/E-5380/MA-srPP-1	753 ~ 50$(G_a)_2$	CF/AIF
LMW-hPP-2/E-5380/MA-srPP-3	896	CF
LMW-hPP-2/E-5380/srPP-4	17.5	AIF
LMW-hPP-2/E-5380/MA-srPP-4	2041	CF
LMW-hPP-2/E-5380/srPP-5	45.5	AIF
LMW-hPP-2/E-5380/MA-srPP-5	4207	AIF/CF
LMW-hPP-2/E-5380/srPP-6	7	AIF
LMW-hPP-2/E-5380/MA-srPP-6	4820 ~ 350$(G_a)_2$	CF

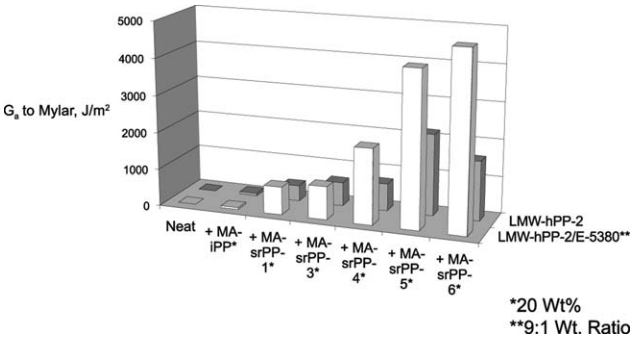

Figure 4. Molecular weight effects of MA-srPP on adhesion to Mylar.

Migration of a particular component in a formulated adhesive to a given contacting surface has been observed before. The wax in an EVA/tackifier/wax hot melt adhesive (HMA) migrates preferentially to the HMA/air interface, but distributes in various degrees at the HMA/polyolefin substrate interface.[35] For a HMA containing a high wax level (33 wt %) bonded to various polyolefin surfaces, the HMA/substrate interfacial composition depends on the wax/substrate compatibility. No weak boundary layer (WBL) of wax appears to exist at the HMA/untreated iPP, HMA/corona-discharge-treated iPP or HMA/corona-discharge-treated PE interface. However, the wax could be enriched at the HMA/untreated PE interface possibly due to a better wax/untreated PE compatibility. Therefore, wax distribution in a HMA depends on the chemical nature of the bonded substrate. Recently, we studied three HMAs based on EVA, tackifier, and wax, the variable being the type of tackifier.[36] Two functional tackifiers and one non-functional tackifier were chosen. By using XPS and ToF-SIMS, we examined the interfacial compositions of these HMAs in contact with air and with Mylar, either under pressure or no pressure. Our findings were that EVA or functional tackifier dominates HMA/Mylar interfaces, but wax dominates the HMA/air interface. This is consistent with the high temperature (150°C) XPS data of the molten HMA surfaces. Based on ToF-SIMS analysis, the HMA surface composition or degree of interfacial segregation depends on the type of tackifier used in the HMA. Overall, a higher concentration of functional tackifier and/or EVA at the HMA/Mylar interface results in a higher adhesion to Mylar. Therefore, it should not

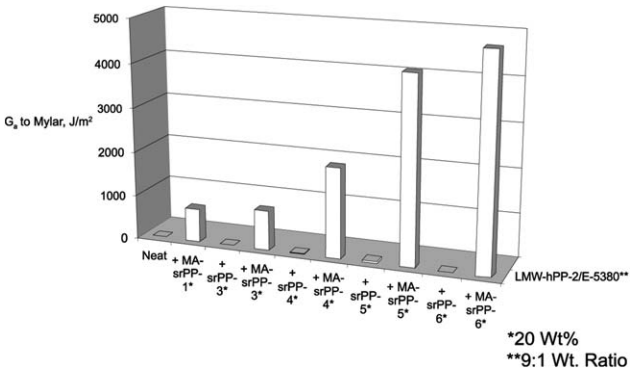

Figure 5. Effects of MA group on adhesion to Mylar.

Table IX. Adhesion Model [eq. (1)], $P = P_oBD$, Used as Guiding Hypothesis

Adhesive Substrate	LMW-hPP/srPP iPP		LMW-hPP/MA-srPP iPP		LMW-hPP/srPP Mylar		LMW-hPP/MA-srPP Mylar
P_o		~		>		<	
B		~		>		~	
D		~		~		~	
P	High		High		Low		High

be too surprising that Mylar can induce the migration of MA groups in the blend of LMW-hPP/MA-srPP to the interface.

Bond Strength with iPP Substrate

In the tie layer application, the adhesive polymer should have high adhesion to both a polar substrate, such as Mylar, and a non-polar substrate, such as iPP. The blend of LMW-hPP/MA-srPP could be a candidate material, as explained by our adhesion model[1–3] in Table IX, where we assume: (1) the same LMW-hPP is used and (2) srPP and MA-srPP have the same molecular weight. For bonding to iPP substrate, P_o, B, and D in eq. (1) should be similar no matter whether srPP or MA-srPP is used in the blend. The resultant adhesion, P, should be high because essentially a propylene-based polymer is adhered to another propylene-based polymer. However, the P_o term for LMW-hPP/srPP or LMW-hPP/MA-srPP to iPP should be higher than that of LMW-hPP/srPP to Mylar because the former adhesive has similar structure and/or similar surface tension as the substrate. Also, we speculate that the B term for LMW-hPP/srPP or LMW-hPP/MA-srPP to iPP should be higher than that of LMW-hPP/srPP to Mylar because iPP has a lower T_m than Mylar. The equilibrium T_m^o of iPP is 208°C, whereas that of poly(ethylene terephthalate) is 282°C.[37] On the other hand, the P_o term for LMW-hPP/MA-srPP with Mylar should be higher than that of LMW-hPP/srPP with Mylar because the former adhesive is more polar. We expect the B and D terms for bonding LMW-hPP/srPP or LMW-hPP/MA-srPP with Mylar should be similar. Therefore, for bonding with Mylar, the higher P_o of LMW-hPP/MA-srPP to Mylar will result in a high adhesion, P, than LMW-hPP/srPP.

The data in Table X appear to be consistent with the hypothesis described in Table IX. The blend of LMW-hPP-2/E-5380/srPP-3 has a poor adhesion to Mylar but a good adhesion to iPP. On the other hand, the blend of LMW-hPP-2/E-5380/MA-srPP-1 has good adhesion to both Mylar and iPP. When the failure mode is denoted as "bond remained intact," only the substrate was elongated and eventually broken with no bond separation at all. The latter, potential tie layer adhesive also outperforms the blend of LMW-hPP-2/E-5380/MA-iPP. Therefore, MA-srPP improves adhesion of LMW-hPP to Mylar without sacrificing adhesion to iPP. The above adhesion behavior is true for the case of functionalized polymers when used alone, as shown in the middle part of Table X, even though MA-iPP has the lowest molecular weight and the highest MA content compared to MA-srPPs. All the MA-srPPs have higher adhesion to both Mylar and iPP than MA-iPP. Again, one notes that MA-srPP is amorphous but MA-iPP is semi-crystallized. Their interaction strengths or the P_o terms with a polar substrate may be different as discussed in the SFG spectroscopic results.

We speculate that both the crystallinity and molecular weight could affect the D term of our adhesion model. A quick and qualitative way to assess the D term of the adhesive[2,4] is to study its stress–strain curve (Figure 6) where the values in parenthesis next to each formulation represent the adhesion to Mylar and iPP (Table X). Normally an adhesive with a low yield

Table X. Bonding of Modified LMW-hPP-2, MA-iPP, MA-srPPs, and MA-RPPs with Mylar and iPP

	G_a to Mylar (J/m^2)	Failure mode	G_a to iPP (J/m^2)	Failure mode
LMW-hPP-2/MA-iPP	70	CF	1015	CF
LMW-hPP-2/E-5380/MA-iPP	49	CF	1005	CF
LMW-hPP-2/E-5380	14	AIF	1082	CF
LMW-hPP-2/E-5380/srPP-3	31.5	AIF	>3609	BRI
LMW-hPP-2/E-5380/MA-srPP-1	753	CF/AIF	>2986	BRI
MA-iPP	1.75	AIF	1278	CF
MA-srPP-3	2310	CF	2002	CF
MA-srPP-4	2846	CF	2730	CF
MA-srPP-5	581	AIF	3910	CF
MA-srPP-6	907	AIF	>2086	BRI
MA-RPP-1	3452	AIF	7907	SE
MA-RPP-4	5226	CF	7648	CF
MA-RPP-5	400.1	AIF	8330	SE

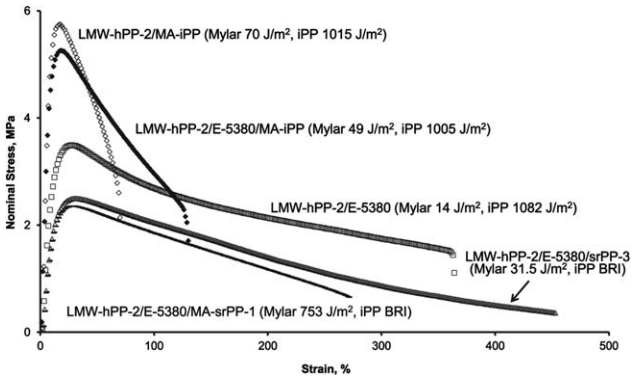

Figure 6. Stress–strain behaviors of LMW-hPP blend compositions.

stress or low crystallinity, a high tensile strength, and a high strain at break (or a large area under the stress–strain curve) will have a high D term.[4] LMW-hPP-2/E-5380/srPP-3 in Figure 6 should have the highest D term. In addition, it has similar structure and/or surface tension as the iPP substrate, producing a high P_o term. Therefore, adhesion to iPP will be high. On the other hand, despite its high D, adhesion to Mylar is low due to a low P_o, as discussed before. LMW-hPP-2/E-5380/MA-srPP-1 in Figure 6 has a lower D (smaller area under the stress–strain curve) than LMW-hPP-2/E-5380/srPP-3 possibly because the molecular weight of MA-srPP-1 is about half that of srPP-3 (Table IV). It has a higher adhesion to Mylar mainly due to its higher P_o compared to the formulation without any MA groups. When bonded to the iPP substrate, the MA groups in LMW-hPP-2/E-5380/MA-srPP-1 stay in the bulk and the iPP substrate is essentially in contact with the non-polar components of the adhesive. Under these conditions, both P_o and B are high, resulting in a high adhesion to iPP. The other compositions in Figure 6 show higher yield stresses due to their higher crystallinities. Although the two compositions containing MA-iPP have smaller areas under the stress-strain curves, they exhibit slightly higher adhesion to Mylar than LMW-hPP-2/E-5380, again probably due a stronger interfacial adhesion P_o between the MA groups and the Mylar substrate. On the other hand, the slightly higher adhesion of LMW-hPP-2/E-5380 to iPP compared to the two compositions containing MA-iPP is attributed to the ductility of the former adhesive, even though all three adhesives should have similar P_o to the iPP substrate.

To understand the molecular weight effects of MA-srPP on adhesion, we revisit Table VIII and Figure 5 and observe that the bond strength of LMW-hPP-2/E-5380/MA-srPP with Mylar increases with increasing molecular weight of MA-srPP. Again, we speculate that P_o remains approximately constant but B may drop with increasing molecular weight of MA-srPP. However, an increase in the molecular weight of MA-srPP increases D. The result is an increase in P according to eq. (1).

LMW-hPP with Low Crystallinity

MA-srPPs are also added to LMW-hPP-6 with a low ΔH_u blended with E-5380 and adhesion of these compositions is studied (Table XI). High adhesion to Mylar has been observed. Also, similar to the results in Figure 5 for LMW-hPP-2 with a higher ΔH_u, adhesion of these LMW-hPP-6 compositions

Table XI. Adhesion of Compositions Based on LMW-hPP-6 (LMW-hPP-6/E-5380/Polymer Modifier = 72/8/20 wt Ratio) to Mylar

	G_a (J/m^2)	Failure mode
LMW-hPP-6	24.5	CF
LMW-hPP-6/E-5380 (9 to 1 wt Ratio)	66.5	CF
LMW-hPP-6/E-5380/MA-srPP-3	1512	CF
LMW-hPP-6/E-5380/MA-srPP-4	2429	CF
LMW-hPP-6/E-5380/MA-srPP-5	3885	CF
LMW-hPP-6/E-5380/MA-srPP-6	4200	CF

increases with increasing molecular weight of MA-srPP. However, failure mode of each bond is CF possibly because of the low molecular weight and/or low viscosity of LMW-hPP-6.

Effects of MA-srPP Content on Adhesion to Mylar

Thus far, the MA-srPP content in LMW-hPP is kept at 20 wt %. It is interesting to see the change in adhesion to Mylar if the MA-srPP content is below 20 wt %. Figure 7 shows the adhesion of two LMW-hPPs with different molecular weights and crystallinities loaded with 1, 5, 10, 15, and 20 wt %'s of MA-srPP-6 to Mylar. Adhesion diminishes with decreasing amounts of MA-srPP. The drop is more severe for LMW-hPP with a lower molecular weight or Brookfield viscosity. At this point, the lower adhesion is attributed to a lower interfacial adhesion (P_o) or a lower debonding term (D) or both. A lower interfacial adhesion (P_o) may be due to an insufficient amount of MA groups at the interface. A lower debonding term (D) is due to a lower quantity of the relatively higher-molecular-weight, amorphous MA-srPP in the composition for enhancing the bulk energy dissipative effects.

Bond Strength of RPP Composition

When 20 wt % of an MA-RPP is added to LMW-hPP, it functions like an adhesion promoter for this polymer, as shown in Table XII and Figure 8. In Table XII, the number to the right-hand-side of each formulation ingredient represents the weight of this ingredient in grams. It is not clear why MA-RPP-4, after formulated with LMW-hPP and E-5380, does not show good adhesion, especially for bonding with Mylar. Overall, we observe

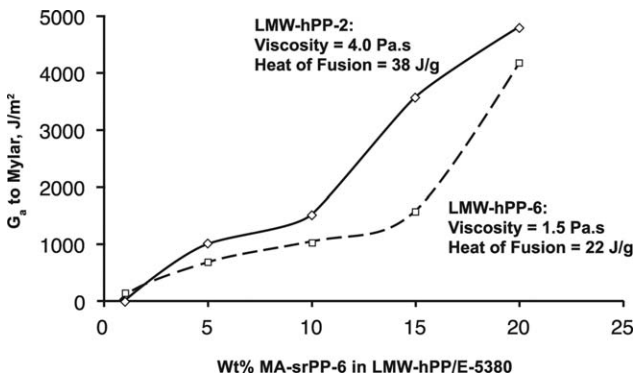

Figure 7. Effects of wt % MA-srPP-6 in LMW-hPP/E-5380 (9 : 1 wt ratio) blend on adhesion to Mylar.

Table XII. Adhesion of LMW-hPP Blended with E-5380 and RPP or MA-RPP

Formulation	Control	Control	Improved Composition	Control	Improved Composition	Control	Improved Composition
LMW-hPP-7	90	72	72	72	72	72	72
E-5380	10	8	8	8	8	8	8
RPP-1	–	20	–	–	–	–	–
MA-RPP-1	–	–	20	–	–	–	–
RPP-2	–	–	–	20	–	–	–
MA-RPP-4	–	–	–	–	20	–	–
RPP-3	–	–	–	–	–	20	–
MA-RPP-5	–	–	–	–	–	–	20
G_a to Mylar (J/m^2)							
After 12 h	17.5[a]	32.2[a]	4340[d]	34.0[a]	895[d]	18.6[a]	4295[d]
After 2 Weeks	9.45[a]	16.8[a]	6339[d]	26.3[a]	2525[a]	7.00[a]	3493[c]
G_a to iPP (J/m^2)							
After 12 h	1408[d]	1524[a]	2423[d]	2604[b]	1302[a]	5989[d]	1621[d]
After 2 Weeks	1263[d]	1519[d]	3068[a]	3403[d]	1199[a]	6066[d]	1439[a]

[a] AIF.
[b] CF/AIF
[c] AIF/CF
[d] CF

high adhesion no matter whether the bond was conditioned for 12 h or 2 weeks.

Adhesion of neat RPPs and MA-RPPs to different substrates is shown in Table XIII and Figure 9. In Table XIII, the abbreviation SE denotes "substrate elongated," in which the substrate was elongated when the bond was opened at the same time. MA-RPPs adhere strongly to polar Mylar or aluminum and non-polar iPP compared to RPPs, which only bond well with iPP. Adhesive strengths after the bonds were conditioned overnight and for 2 weeks are reported. It appears that the lower-crystallinity MA-RPP (MA-RPP-1 or MA-RPP-4 with a higher C_2 content) adheres to Mylar better, similar to the behaviors of MA-srPP versus MA-iPP. On the other hand, they all bond well with aluminum. Both RPP and MA-RPP crystallize slowly. Overall, adhesive strength increases slightly for each of these bonds after it was conditioned for 2 weeks and some bonds exhibit changes in failure mode. Table XIII also shows the stress–strain properties of RPPs and MA-RPPs, where the toughness is defined as the area under the stress–strain curve. After maleation, RPP-1 shows a decrease in tensile strength, consistent with the GPC results that MA-RPP-1 has lower molecular weights than RPP-1. MA-RPP-5 is the only polymer showing a yield point. Based on Table IV, it has a higher level of crystallinity because it has the lowest C_2 content and exhibits both higher T_m and ΔH_u than the other RPPs and MA-RPPs.

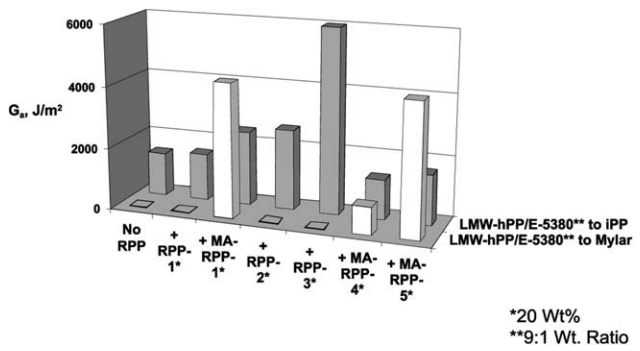

Figure 8. Adhesion of LMW-hPP blended with E-5380 and RPP or MA-RPP to Mylar and iPP after conditioned for 12 h.

Neat MA-RPPs adhered to both Mylar and iPP are compared to the neat MA-iPP and MA-srPPs in Table X, where all bonds have been conditioned for 12 h before the T-peel measurements. It is obvious that both MA-srPPs and MA-RPPs outperform MA-iPP.

SFG Spectroscopy

Polymer/Alumina Interface: CH Region. Because SFG spectroscopy is highly sensitive to the molecular arrangement at an interface,[38] one could detect any variation in molecular arrangement at the polymer/alumina interface caused by the migration of functionality towards the interface. We use SFG in the range of 2800–3000 cm^{-1} to monitor spectral features at the interface between alumina and LMW-hPP-2, MA-srPP-1, and LMW-hPP-2/MA-srPP-1. In all the blends for SFG study, only LMW-hPP-2, MA-srPP-1, and MA-iPP are used and the functionalized polymer content is always kept at 20 wt %. The SFG results for LMW-hPP, MA-srPP, and their blend are depicted in Figure 10, where aPP-iPP ≡ LMW-hPP. Even a cursory inspection of the data shows that the molecular arrangements at the interface between MA-srPP and alumina and that between LMW-hPP/MA-srPP and alumina are identical. However, these are markedly different from the interface between LMW-hPP and alumina. These results indicate that the interface between LMW-hPP/MA-srPP and alumina has the same characteristic as the

Table XIII. Adhesion of Neat RPP and MA-RPP

Polymer	RPP-1 (Control)	MA-RPP-1	RPP-2 (Control)	MA-RPP-4	RPP-3 (Control)	MA-RPP-5
G_a to Mylar (J/m^2)						
After 12 h	14.7[a]	3452[a]	31.5[a]	5226[b]	37.1[a]	400.1[a]
After 2 weeks	4.90[a]	3920[a]	13.7[a]	5835[b]	4.55[a]	944.3[a]
G_a to Al (J/m^2)						
After 12 h	86.1[a]	10336[a]	90.0[a]	15477[b]	58.8[a]	18172[b]
After 2 weeks	0[a]	12740[a]	0[a]	>14000[d]	0[a]	>14000[d]
G_a to iPP (J/m^2)						
After 12 h	7035[b]	7907[c]	6787[b]	7648[b]	7147[b]	8330[c]
After 2 weeks	7294[b]	8610[a]	6710[b]	6269[b]	7721[b]	8974[a]
Yield stress (MPa)						4.14
Yield strain (%)						32
100% Modulus (MPa)	1.86	1.60	2.32	1.55	1.63	3.99
Tensile strength (MPa)	14.1	8.40	13.2	5.73	8.46	11.9
Strain at break (%)	950	1070	1000	1010	770	770
Toughness (10^6J/m^3)	77	63	89	47	42	74

[a] AIF
[b] CF
[c] SE
[d] BRI

interface between MA-srPP and alumina, suggesting the migration of MA-srPP towards the alumina surface.

Since inferring the migration of MA-srPP towards the interface from the molecular arrangement is a qualitative observation, one cannot obtain any information regarding the strength of the interaction between the polymer and substrate. In order to examine these interfaces using a more quantitative method, we have studied the above interfaces in the 1650–1900 cm^{-1} range. These systems were also compared to the interface between LMW-hPP/MA-iPP and alumina.

Polymer/Alumina Interface: C=O Region. MA-srPP, MA-iPP, and MA-RPP contain the C=O moiety with a vibrational resonance frequency in the range of 1700–1800 cm^{-1}. The C=O resonance features could be detected with SFG and used as evidence of the existence of MA-srPP, MA-iPP, and MA-RPP at the polymer/alumina interface. However, we should note that the generation and detection of SFG in the 1700 cm^{-1} range is accompanied by various difficulties that must be overcome. For example, an alumina prism adsorbs IR in this range causing a significant reduction in the infrared intensity before reaching the interface. In addition, other non-adsorbing and isotropic high-surface-energy prism materials do not have a large enough index of reflection suitable for SFG measurements in the total internal reflection geometry. We have overcome this difficulty by using an equilateral alumina (sapphire) prism and keeping the beam close to the vertex where the optical path for the IR input beam is minimal. In addition to prism adsorption, the IR beam also contains sharp spectral bands due to ambient water adsorption. To avoid any artifacts due to the ambient water, we have purged the

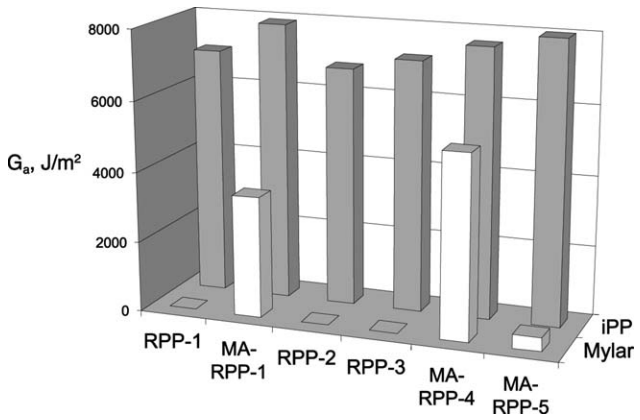

Figure 9. Adhesion of neat RPP and MA-RPP to Mylar and iPP after conditioned for 12 h.

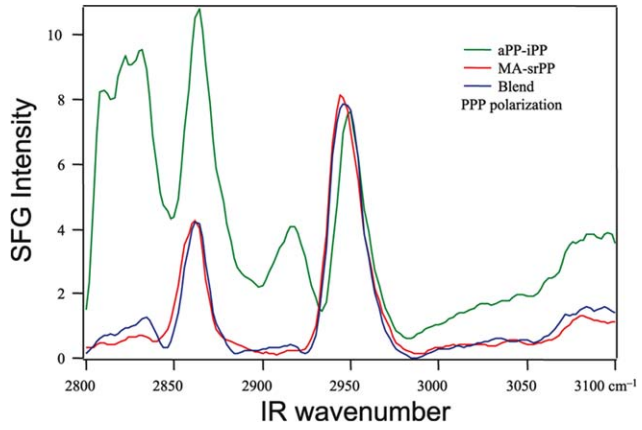

Figure 10. SFG spectra of the interfaces between alumina and LMW-hPP, MA-srPP, and LMW-hPP/MA-srPP in the CH region. [Color figure can be viewed in the online issue, which is available at wileyonlinelibrary.com.]

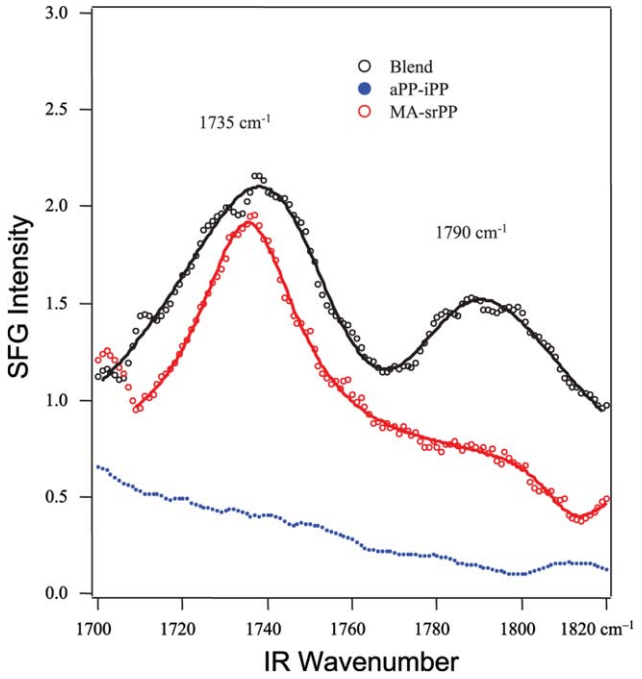

Figure 11. SFG spectra of the interfaces between alumina and LMW-hPP, MA-srPP, and LMW-hPP/MA-srPP in the C=O region. [Color figure can be viewed in the online issue, which is available at wileyonlinelibrary.com.]

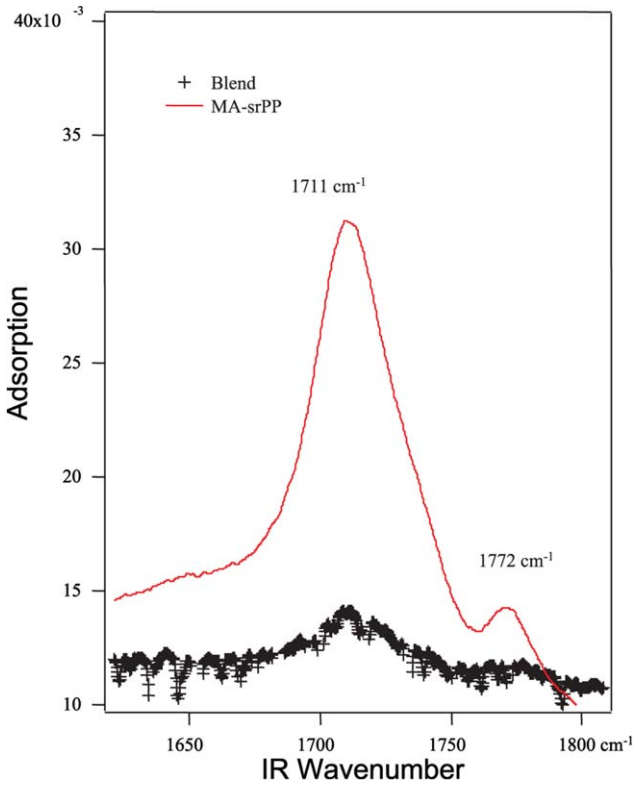

Figure 12. FTIR of MA-srPP and LMW-hPP/MA-srPP in ATIR mode. [Color figure can be viewed in the online issue, which is available at wileyonlinelibrary.com.]

entire sampling area with N_2 and normalized the SFG beam to the infrared input power spectrum. This procedure was successfully tested using known substances possessing the C=O moiety, such as acetone.

Figure 11 shows the SFG spectra of the various interfaces of LMW-hPP, MA-srPP, and LMW-hPP/MA-srPP with alumina, where aPP-iPP ≡ LMW-hPP. As expected, the spectrum of the interface between LMW-hPP and alumina shows no structural features in the range of 1650–1900 cm^{-1}. However, the SFG spectrum of the interface between MA-srPP and alumina shows two structures at ~1735 and 1790 cm^{-1} due to the C=O moiety of MA-srPP, suggesting the existence of MA at the polymer/alumina interface. The spectrum of the interface between LMW-hPP/MA-srPP and alumina also shows the same spectral features. Comparing these spectra one envisions the migration of the functionalized srPP towards the alumina surface to reduce the interfacial energy. The increase in the SFG strength of the 1790 cm^{-1} resonance at the interface between LMW-hPP/MA-srPP and alumina as compared to MA-srPP may be due to better ordering of the polymer at the interface.

It is known that the interaction between functionalities containing C=O and the substrate could produce a frequency shift of this moiety at the polymer/substrate interface.[39] To examine this scenario, we have carried out FTIR of MA-srPP and LMW-hPP/MA-srPP in ATIR mode, shown in Figure 12. There are two structural features observed in the ATIR of these two samples, one at 1711 cm^{-1} and the other at 1772 cm^{-1}. Since the ATIR-FTIR detects those molecules that are in the bulk of the material, we mark the 1711 and 1772 cm^{-1} features as the vibrational resonance of the C=O moiety of a non-interacting MA functionality. As seen in Figures 11 and 12, the SFG peak positions are shifted by approximately 20 cm^{-1} with respect to the features of the non-interacting MA. These frequency shifts are an indication of an interaction between the MA functionality and the high-surface-energy alumina. The interaction between LMW-hPP/MA-srPP and the high-surface-energy substrate increases the P_o parameter in eq. (1) and thus significantly enhances the adhesion between the polymer and high-surface-energy materials, such as Mylar, as observed in the measured work of detachment.

Figure 13 shows the SFG spectra of the two interfaces between MA-iPP and LMW-hPP/MA-iPP with alumina, where aPP-iPP ≡ LMW-hPP. There is a strong resonance peak at 1710 cm^{-1} and a weak peak at 1790 cm^{-1} which indicate the existence of MA-iPP at the polymer/alumina interface. These results reveal that the MA-iPP also migrates to the surface of alumina to reduce the interfacial surface energy. We compare the SFG spectra of the various interfaces between MA-srPP, LMW-hPP/MA-srPP, and LMW-hPP/MA-iPP with alumina to the ATIR of the bulk MA-srPP in Figure 14, where aPP-iPP ≡ LMW-hPP. The peak position of the C=O moiety in LMW-hPP/MA-iPP is very close to the peak position of C=O in the bulk, indicating little or no interaction between this material and the alumina substrate. On the other hand, the C=O peak position is shifted in MA-srPP, suggesting an interaction between MA-srPP and alumina (Figures 11 and 12). This difference in the strength of the

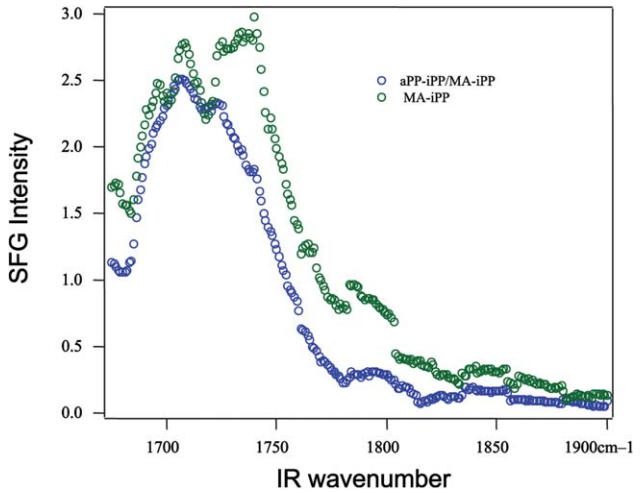

Figure 13. SFG spectra of the interfaces between alumina and MA-iPP and LMW-hPP/MA-iPP in the C=O region. [Color figure can be viewed in the online issue, which is available at wileyonlinelibrary.com.]

interaction between the polymer and a high-energy solid substrate causes differences in the adhesive strength as observed in peel adhesion measurements, in addition to the difference in the debonding term (D; Figure 6).

The difference in the interaction strength for MA-srPP versus MA-iPP with sapphire is not fully understood and needs to be determined. It could be due to the ease of molecular rearrangement of MA groups in the more amorphous srPP environments or due to some other local effect.

Similarly, the C=O resonance features of MA-RPP could be detected with SFG and used as evidence of the existence of MA functionality at the MA-RPP/alumina interface. This system was also compared to the RPP/alumina interface, which shows, as expected, no structural features between 1650–1900 cm^{-1} (Figure 15). However, the spectrum of MA-RPP/alumina shows two structures at ~1735 and 1772 cm^{-1}. These two peaks are due to the C=O moiety of MA-RPP and are indicative of the existence of

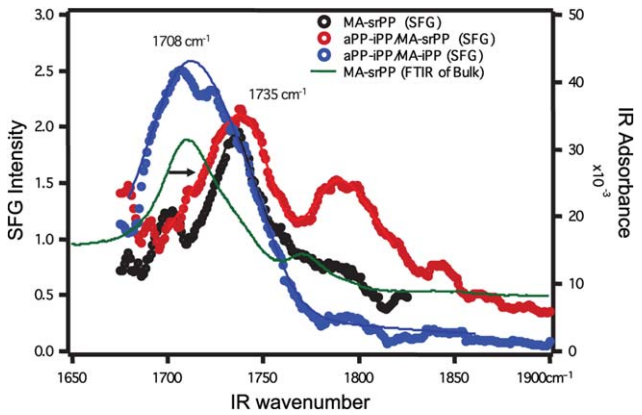

Figure 14. Comparison of the SFG spectra of the interfaces between MA-srPP, LMW-hPP/MA-srPP, and LMW-hPP/MA-iPP with alumina to the ATIR spectrum of the bulk MA-srPP in the C=O region. [Color figure can be viewed in the online issue, which is available at wileyonlinelibrary.com.]

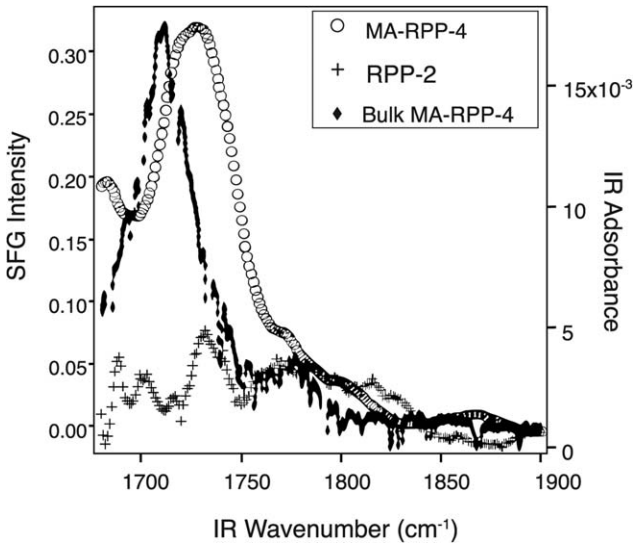

Figure 15. Comparison of the SFG spectra of the MA-RPP/alumina and RPP/alumina interfaces to the ATIR spectrum of the bulk MA-RPP in the C=O region.

MA groups at the polymer/alumina interface. Comparing these spectra one concludes the migration of MA functionality towards the alumina surface to reduce the interfacial energy.

Similar to our approach on MA-srPP, we have also carried out FTIR of MA-RPP-4 (the MA-RPP with the lowest ΔH_u) in ATIR mode, also shown in Figure 15. There are two structural features observed in the ATIR of this sample, one at 1711 cm^{-1} and the other at 1772 cm^{-1}. Since the ATIR–FTIR detects those molecules that are in the bulk of the material, we mark the 1711 and 1772 cm^{-1} features as the vibrational resonance of the C=O moiety of a non-interacting MA functionality. As seen in Figure 15, the major SFG peak at 1735 cm^{-1} is shifted by approximately 20 cm^{-1} with respect to the features of the non-interacting MA. This frequency shift suggests interactions between the MA functionality and the high-surface-energy alumina. Similar to the previous discussion for MA-srPP, the interaction between MA-RPP and the high-surface-energy substrate increases the P_o parameter in eq. (1) and thus significantly enhances the adhesion between the polymer and high-surface-energy materials, such as Mylar or aluminum, as observed in peel adhesion measurements.

CONCLUSIONS

Conclusions derived from this study on the modification of LMW-hPP by MA-srPP or MA-RPP are:

- MA functionalized srPP or RPP improves LMW-hPP adhesion to polar substrates, such as Mylar, due to the higher interfacial attraction [enhanced P_o in eq. (1)] between the modified LMW-hPP adhesive and the polar Mylar substrate.
- Compared to MA-iPP, MA-srPP shows (50–350)× and (40–200)× increases in bond strength with Mylar for LMW-hPP/MA-srPP blends with and without a tackifier, respectively. Also, the adhesion of these blends to iPP remains high.

- When utilized alone as an adhesive to Mylar and iPP, both MA-srPP and MA-RPP outperform MA-iPP (Table X).
- Our adhesion model, $P = P_oBD$, provides a successful framework for understanding the adhesive bonding with Mylar and iPP substrates in the tie layer applications; this model is also useful for guiding the development of new adhesives.
- The buried interface between the LMW-hPP/MA-srPP blend (80 to 20 wt ratio) and sapphire has the same SFG characteristic spectrum as the MA-srPP/sapphire interface, suggesting the enrichment of MA groups in the interfacial polymer. Vibrational modes of C=O have been detected at both the blend/sapphire and MA-srPP/sapphire interfaces. This further indicates the possibility of the interfacial polymer containing MA groups.
- SFG studies indicate that MA-srPP or MA-RPP with zero or lower crystallinity interacts more strongly with sapphire than MA-iPP, suggesting a higher P_o term of MA-srPP or MA-RPP to Mylar than MA-iPP.

Presently we are studying the structure–property–adhesion relations of a number of low-molecular-weight versions of RPP and their blends. We are attempting to introduce a new adhesion polymer with lower viscosity to the industry.

ACKNOWLEDGMENTS

I wish to thank H. Wakabayashi of Tonen Chemical Company for the solution-maleation of some srPPs, J.-R. Schauder for the melt-maleation of RPPs, M. S. Yeganeh and S. M. Dougal for SFG measurements and analysis, C. J. Ruff for ^{13}C NMR measurements, P. Jiang and C. Gong for supplying some of the polymers, and J. Li for experimental assistance.

REFERENCES

1. Tse, M. F. *J. Adhesion Sci. Technol.* **1989**, *3*, 551.
2. Tse, M. F. *J. Adhesion* **1995**, *48*, 149.
3. Tse, M. F.; Jacob, L. *J. Adhesion* **1996**, *56*, 79.
4. Tse, M. F. *Proc Am. Chem. Soc. Div. Polym Mater Sci Eng* **2000**, *82*, 125.
5. Lohse, D. J. *J. Macromol. Sci. Part C: Polym. Rev* **2005**, *45*, 289.
6. Graessley, W. W. Polymeric Liquids & Networks; Taylor & Francis Group, LLC: New York, NY, **2008**.
7. Stehling, F. C.; Mandelkern, L. *Macromolecules* **1970**, *3*, 242.
8. Wu, S. Polymer Interface and Adhesion; Marcel Dekker, Inc.: New York, NY, **1982**.
9. Mori, H.; Hatanaka, T.; Terano, M. *Macromol. Rapid Commun.* **1997**, *18*, 157.
10. Borggreve, R. J. M.; Gaymans, R. *J. Polymer* **1989**, *30*, 63.
11. Montiel, A, G.; Keskkula, H.; Paul, D. R. *Polymer* **1995**, *36*, 4605.
12. Cho, K; Seo, K. H.; Ahn, T. O.; Kim, J; Kim, K. U. *Polymer* **1997**, *38*, 4825.
13. Bikiaris, D.; Matzinos, P.; Larena, A; Flaris, V.; Panayiotou, C. *J. Appl. Polym. Sci.* **2001**, *81*, 701.
14. Zhao, R.; Dai, G. *J. Appl. Polym. Sci.* **2002**, *86*, 2486.
15. Chakrit, S.; Sauvarop, L.; Jarunee, T. *J. Appl. Polym. Sci.* **2003**, *89*, 1156.
16. Purnima, D.; Maiti, S. N.; Gupta, A. K. *J. Appl. Polym. Sci.* **2006**, *102*, 5528.
17. Kim, H.-S.; Lee, B.-H; Choi, S.-W.; Kim, S.; Kim, H.-J. *Composites: Part A* **2007**, *38*, 1473.
18. El-Wakil, A. A. *Int. J. Polym. Sci.* **2011**, Article ID 591948.
19. Lee, Y.; Char, K *Macromolecules* **1994**, *27*, 2603.
20. Sun, T.; Brant, P.; Chance, R. R.; Graessley, W. W. *Macromolecules* **2001**, *34*, 6812.
21. Sclavons, M.; Franquinet, P.; Carlier, V.; Verfaillie, G.; Fallais, I.; Legras, R.; Laurent, M.; Thyrion, F. C. *Polymer* **2000**, *41*, 1989.
22. Bu, H.-S.; Cheng, S. Z. D.; Wunderlich, B. *Makromol. Chem. Rapid Commun.* **1988**, *9*, 75.
23. Cheng, H. N. *Macromolecules* **1984**, *17*, 1950.
24. Imuta, J.; Ueda, T.; Kiso, Y.; Mizuno, A.; Kawasaki, M.; Hashimoto, M. US Patent No. 5,504,172.
25. Tsutsui, T.; Ishimaru, N.; Mizuno, A.; Toyota, A.; Kashiwa, N. *Polymer* **1989**, *30*, 1350.
26. Schauder, J.-R.; Datta, S. WO 02/36651 A1.
27. Tse, M. F. *Proc. Am. Chem. Soc. Div. Polym. Mater. Sci. Eng.* **2005**, *92*, 409.
28. Polymers Grade Slate for Adhesives & Sealants, ExxonMobil Chemical Company, **2001**.
29. Martuscelli, E.; Silvestre, C.; Canetti, M.; de Lalla, C.; Bonfatti, A. M.; Seves, A. *Markromol. Chem.* **1989**, *190*, 2615.
30. Martuscelli, E.; Canetti, M.; Seves, A. *Polymer* **1989**, *30*, 304.
31. Martuscelli, E.; Canetti, M.; Bonfatti, A. M.; Seves, A. *Polymer* **1991**, *32*, 641.
32. Tse, M. F.; Hu, W.; Yeganeh, M. S.; Zhang, D. *J. Appl. Polym. Sci.* **2004**, *93*, 323.
33. Yeganeh, M. S.; Dougal, S. M.; Polizzotti, R. S.; Rabinowitz, P. *Thin Solid Films* **1995**, *270*, 226.
34. Rabinowitz, P.; Perry, B. N.; Levinos, N. *Quantum Electron* **1986**, *22*, 797.
35. Tse, M. F. *J. Adhesion* **1998**, *66*, 61.
36. Tse, M. F. *Proc. Am. Chem. Soc. Div. Polym. Mater. Sci. Eng.* **2006**, *94*, 564.
37. Mark, J. E.; Eisenberg, A.; Graessley, W. W.; Mandelkern, L.;Samulski, E. T.; Koenig, J. L.; Wignall, G. D. Physical Properties of Polymers, 2nd ed.; Am. Chem. Soc.: Washington, DC, **1993**.
38. Gautam, K. S.; Schwab, A. D.; Dhinojwala, A.; Zhang, D.; Dougal, S. M.; Yeganeh, M. S. *Phys. Rev. Lett.* **2000**, *85*, 3854.
39. Sim, W.; Li, T.; Yang, P.; Yeo, B. *J. Am. Chem. Soc.* **2002**, *124*, 4970.